Karlsruhe Institute of Technology

Institute for Theoretical Particle Physics

Phenomenology of flavoured dark matter

MU Programmtag 2016, Mainz

Monika Blanke, **Simon Kast** | Dez 12, 2016

KARLSRUHE INSTITUTE OF TECHNOLOGY

Outline

Simplified Models

- Presence of Dark Matter ($\Omega_{DM} \approx 27\%$) demands extension of Standard Model (SM).
  $\rightarrow$ What can we do to find the right extension?
- One extreme: full theory extension of SM (e.g. SUSY).
- Other extreme: effective field theory (EFT) approach.
- The middle way: simplified models.
- Advantage of simplified models: Study specific interactions with limited number of parameters.

The Flavour Gate to Dark Matter

Karlsruhe Institute of Technology

Assume an analogy to the SM fermions $\rightarrow$ dark flavour triplet χ_i.

The Flavour Gate to Dark Matter

Assume an analogy to the SM fermions $\rightarrow$ dark flavour triplet χ_i.

Flavoured Dark Matter coupling to SM right-handed up-quark triplet:

$$\mathcal{L}_{\text{NP,int}} = -\lambda_{ij}\bar{u}_{Ri}\chi_j\phi + h.c.$$

- DM flavour triplet χ_j, Dirac fermion, SM gauge singlet.
- Heavy scalar mediator ϕ, carrying colour and hypercharge.
- Lagrangian has unbroken $\mathbb{Z}_3$ symmetry and hence yields stability of DM χ (for $m_\phi > m_\chi$).

Dark Minimal Flavour Violation

[Agrawal, Blanke, Gemmler '14]

Flavour Symmetry

$$U(3)_u \times U(3)_d \times U(3)_q \times U(3)_\chi$$

is only broken by SM Yukawa couplings and the DM-quark coupling λ_{ij} (Dark Minimal Flavour Violation).

$\Rightarrow$ only DM mass splitting comes from RG running:

$$m_{ij} = m_\chi(\mathbb{1} + \eta\lambda^\dagger\lambda + ...)_{ij}.$$

- η depends on the full theory $\rightarrow$ has to be a parameter of the simplified model.
- flavour with lowest mass is our DM candidate.
  $\rightarrow$ we choose the "top-flavour". [Kilic, Klimek, Yu '15]

Parametrization of DM-Quark Coupling Matrix

After using all the symmetries at our disposal λ has 9 parameters left and can be parametrized as:

$$\lambda = U_{23}^{\lambda} U_{13}^{\lambda} U_{12}^{\lambda} D_{\lambda}$$

- D_{λ} is a real diagonal matrix $D_{\lambda} = \text{diag}(D_{\lambda,11}, D_{\lambda,22}, D_{\lambda,33})$.
- U_{ij}^{λ} are unitary matrices with mixing angles Θ_{ij} and phases δ_{ij}.

$\Rightarrow$ new source of flavour <u>and</u> CP violation

How to Detect Flavoured Dark Datter?

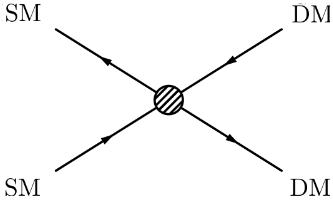

collider searches

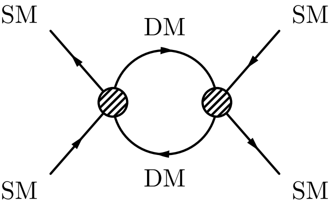

precision flavour data

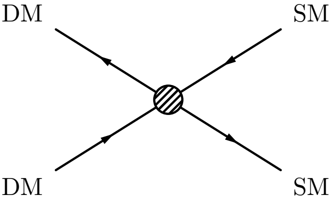

indirect detection / freeze-out

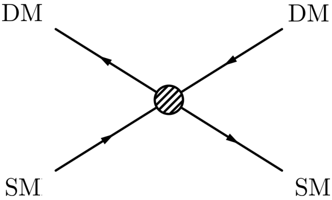

direct detection

Constraints from SUSY Searches at LHC

Constraints from SUSY-searches ($t\bar{t}$ or dijet final states)
[ATLAS collaboration '14]

Study $pp \to \phi\bar{\phi} \to q\bar{q}\chi\bar{\chi}$

- Production either through $g\phi\bar{\phi}$ or NP interaction (coupling-dependent).
- Decay either to top or jet ($+ \not{E}_T$).

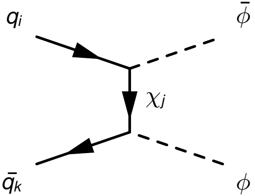

Figure : NP interaction production channel.

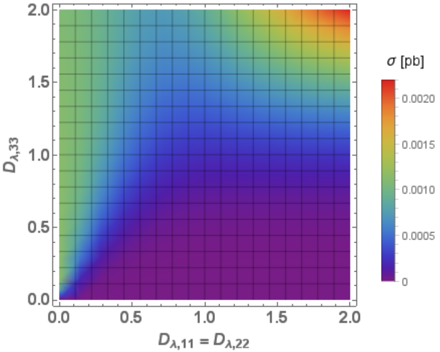

Figure : Cross section for $t\bar{t}$ final state, mixing angles set to zero, $m_\phi = 850$ GeV and $m_\chi = 50$ GeV.

Constraints from SUSY Searches at LHC

[ATLAS collaboration '14]

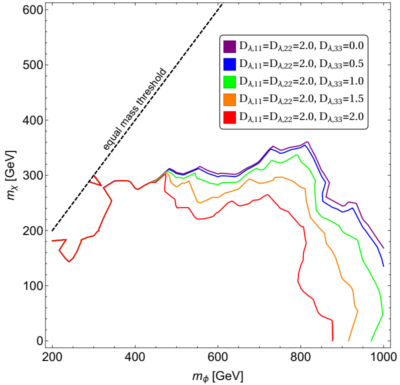

Figure : Exclusion plot for dijet final state, mixing angles set to zero.

- The phenomenologically interesting region is $m_\chi \leq 1$ TeV.
- Too large couplings $D_{\lambda,ii}$ would exclude nearly all of parameterspace.
- Most serious constraints come from dijet final state.

$\Rightarrow$ Safe parameter-space:

$$m_\phi \geq 850 \text{ GeV}$$

$$2.0 \geq D_{\lambda,33} > D_{\lambda,22}, D_{\lambda,11}$$

$\Rightarrow$ Also safe with mixings allowed.

Flavour Constraints from Neutral Meson Mixing

[UTfit collaboration '14]

- No mesons with top-quark are possible, the only constraints come from D-mesons.
  $\Rightarrow$ not too strong

- The NP contribution has to be smaller than experimental bounds.
  $\Rightarrow$ constraints on mixing angles, mostly Θ_{12}

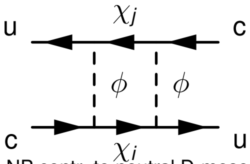

Figure : NP contr. to neutral D-meson mixing.

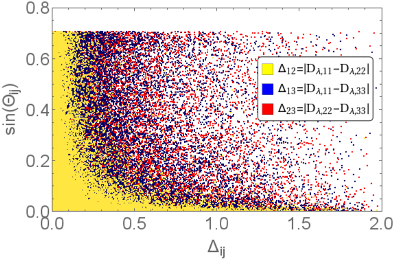

Figure : Valid mixing angles for different coupling splittings. $m_\phi = 850$ GeV and $m_\chi = 250$ GeV.

DM Constraints from Observed Relic Abundance

[Steigman, Dasgupta, Beacom '12]

- Assume DM abundance as a thermal relic.
- Depending on mass-splitting several freeze-out scenarios are possible.
- If DM mass is below top-mass several channels drop out.
  $\Rightarrow$ different impact on parameters
- Co-annihilation has to be just as large as to produce the correct relic density.
  $\Rightarrow$ cuts out valid area for $D_{\lambda,ii}$ depending on m_ϕ and m_χ
- Lower bounds on DM mass depending on mediator mass.
- Depending on η an upper DM bound arises in single-flavour freeze-out scenarios.

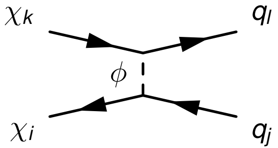

Figure : Co-annihilation of DM flavours.

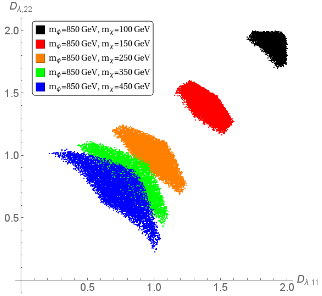

Figure : Valid points in quasi-degenerate freeze-out scenario.

DM Bounds from Direct Detection Experiments

[LUX collaboration '16]

- Many contributions to total WIMP-nucleon cross section, only Z-penguin with neutron is negative.
  $\Rightarrow$ saves the day
- Tree level and neutron Z-penguin have to nearly cancel each other.
  $\Rightarrow$ serious constraints on Θ_{13}
- For too large couplings the cancellation is no longer possible $\rightarrow$ excluded.
- Top-flavoured DM is the natural choice.

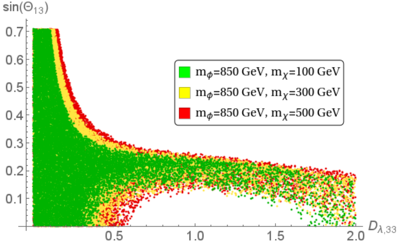

Figure : Valid mixing angle Θ_{13} vs $D_{\lambda,33}$.

Figure : Cancellation of tree-level and neutron Z-penguin contributions (symbolic).

Combined Analysis of Constraints

Karlsruhe Institute of Technology

- The combination of relic abundance and direct detection constraints confines Θ_{13} to a narrow interval around the "perfect" cancellation point.
- The lower and upper bounds on the DM mass become more serious, since the parameters do not only have to fulfill relic abundance constraints.
- The combined analysis clearly prefers top-flavoured DM.

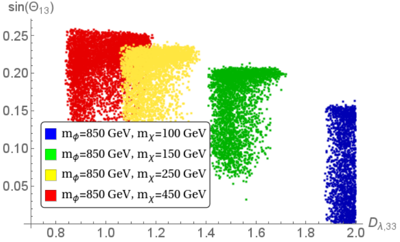

Figure : Valid points in Θ_{13}-$D_{\lambda,33}$-plane (QDF).

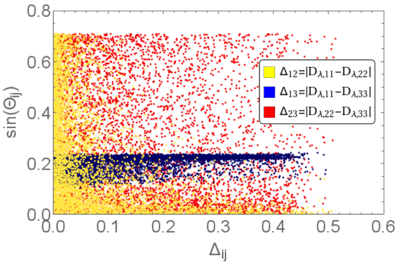

Figure : Valid points for $m_\phi = 850$ GeV and $m_\chi = 250$ GeV (QDF).

Implications of Enhanced Constraints

Xenon has 9 stable or quasi-stable isotopes (7 make up significant fraction of natural Xenon).
⇒ perfect cancellation in DD CS different for isotopes
⇒ for enhanced constraints not always possible

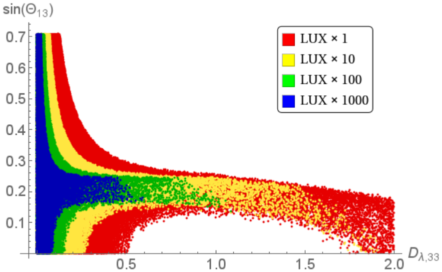

Figure : Valid points for only DD constraints with $m_\phi = 850$ GeV and $m_\chi = 250$ GeV in Θ_{13}-$D_{\lambda,33}$-plane for different strengths of LUX constraints in QDF.

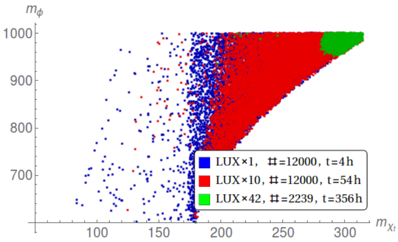

Figure : Valid points in Mass Scan for different strengths of LUX constraints in SFF.

Recap

- A simplified model of flavoured DM coupled to SM right-handed up-quark triplet. Coupling is general following the concept of DMFV.
- Assuming $m_\chi < 1$ TeV (phenomenologically interesting area).
- With this mass the RA constraints demand high $D_{\lambda,ii}$ for high mediator mass m_ϕ.
- High couplings prevent the necessary cancellation in WIMP-nucleon cross section. $\Rightarrow$ Mediator mass can not be too large if $m_\chi < 1$ TeV.
- Collider constraints limit couplings for a reasonable m_ϕ (NP production).
- Constraints from dijet searches prefer $D_{\lambda,33} \geq D_{\lambda,22}, D_{\lambda,11}$.
- Direct detection constraints prefer top-flavoured DM.
- In combination with the limits on couplings, the RA constraints produce a lower bound for the DM mass (depending on m_ϕ).
- In SFF the splitting conditions in combination with RA constraints also establishes an upper bound on m_χ (depending on m_ϕ and η).

Conclusion and Outlook

- All kinds of different constraints $\rightarrow$ multitude of effects and interesting interplay.
- Especially interesting effect on mixing angle θ_{13} due to DD and RA constraints.
  $\Rightarrow$ Future measurements of direct detection experiments will test a large part of the parameter space.
  $\Rightarrow$ Ongoing Xenon experiments or experiments with other noble gases well motivated.
- Simplified models are powerful tool to study diversity of constraints.
- Going beyond Minimal Flavour Violation is worth the effort.
  $\rightarrow$ Dark Minimal Flavour Violation as guidance.

The End

Thank you!

Thank you!

Questions?

References I

Georges Aad et al. "Search for squarks and gluinos with the ATLAS detector in final states with jets and missing transverse momentum using $\sqrt{s} = 8$ TeV proton–proton collision data". In: *JHEP* 09 (2014), p. 176. DOI: 10.1007/JHEP09(2014)176. arXiv: 1405.7875 [hep-ex].

Georges Aad et al. "Search for top squark pair production in final states with one isolated lepton, jets, and missing transverse momentum in $\sqrt{s}$ =8 TeV *pp* collisions with the ATLAS detector". In: *JHEP* 11 (2014), p. 118. DOI: 10.1007/JHEP11(2014)118. arXiv: 1407.0583 [hep-ex].

R Aaij et al. "Precision measurement of D meson mass differences". In: *JHEP* 1306 (2013), p. 065. DOI: 10.1007/JHEP06(2013)065. arXiv: 1304.6865 [hep-ex].

References II

- Prateek Agrawal, Monika Blanke, and Katrin Gemmler. "Flavored dark matter beyond Minimal Flavor Violation". In: *JHEP* 1410 (2014), p. 72. DOI: 10.1007/JHEP10(2014)072. arXiv: 1405.6709 [hep-ph].
- D. S. Akerib et al. "Improved WIMP scattering limits from the LUX experiment". In: (2015). arXiv: 1512.03506 [astro-ph.CO].
- Sinya Aoki et al. "Review of lattice results concerning low-energy particle physics". In: *Eur.Phys.J.* C74 (2014), p. 2890. DOI: 10.1140/epjc/s10052-014-2890-7. arXiv: 1310.8555 [hep-lat].
- A.J. Bevan et al. "The UTfit collaboration average of D meson mixing data: Winter 2014". In: *JHEP* 1403 (2014), p. 123. DOI: 10.1007/JHEP03(2014)123. arXiv: 1402.1664 [hep-ph].

References III

Monika Blanke et al. “FCNC Processes in the Littlest Higgs Model with T-Parity: a 2009 Look”. In: *Acta Phys.Polon.* B41 (2010), pp. 657–683. arXiv: 0906.5454 [hep-ph].

N. Carrasco et al. “$D^0 - \bar{D}^0$ mixing in the standard model and beyond from $N_f = 2$ twisted mass QCD”. In: *Phys.Rev.* D90.1 (2014), p. 014502. DOI: 10.1103/PhysRevD.90.014502. arXiv: 1403.7302 [hep-lat].

Carlos A. Chavez, Ray F. Cowan, and W.S. Lockman. “Charm meson mixing: An experimental review”. In: *Int.J.Mod.Phys.* A27 (2012), p. 1230019. DOI: 10.1142/S0217751X12300190. arXiv: 1209.5806 [hep-ex].

References IV

Csaba Csaki, Adam Falkowski, and Andreas Weiler. "The Flavor of the Composite Pseudo-Goldstone Higgs". In: *JHEP* 0809 (2008), p. 008. DOI: 10.1088/1126-6708/2008/09/008. arXiv: 0804.1954 [hep-ph].

Yuval Grossman, Yosef Nir, and Gilad Perez. "Testing New Indirect CP Violation". In: *Phys.Rev.Lett.* 103 (2009), p. 071602. DOI: 10.1103/PhysRevLett.103.071602. arXiv: 0904.0305 [hep-ph].

Alexander L. Kagan and Michael D. Sokoloff. "On Indirect CP Violation and Implications for D0 - anti-D0 and B(s) - anti-B(s) mixing". In: *Phys.Rev.* D80 (2009), p. 076008. DOI: 10.1103/PhysRevD.80.076008. arXiv: 0907.3917 [hep-ph].

References V

Can Kilic, Matthew D. Klimek, and Jiang-Hao Yu. “Signatures of Top Flavored Dark Matter”. In: *Phys.Rev.* D91.5 (2015), p. 054036. DOI: 10.1103/PhysRevD.91.054036. arXiv: 1501.02202 [hep-ph].

Alexey A Petrov. “Long-distance effects in charm mixing”. In: (2013). arXiv: 1312.5304 [hep-ph].

Gary Steigman, Basudeb Dasgupta, and John F. Beacom. “Precise Relic WIMP Abundance and its Impact on Searches for Dark Matter Annihilation”. In: *Phys.Rev.* D86 (2012), p. 023506. DOI: 10.1103/PhysRevD.86.023506. arXiv: 1204.3622 [hep-ph].

James D. Wells. “Annihilation cross-sections for relic densities in the low velocity limit”. In: (1994). arXiv: hep-ph/9404219 [hep-ph].

Constraints from SUSY Searches at LHC

[ATLAS collaboration '14]

- Study the process
  $pp \to \phi\bar{\phi} \to q\bar{q}\chi\bar{\chi}$.
- Depending on decay product of ϕ we detect either a top-signature or a jet ($+\not{E}_T$).
- Inspiration from SUSY searches at LHC
  $\Rightarrow$ Upper bounds on CS of both $t\bar{t}$ and dijet signals.

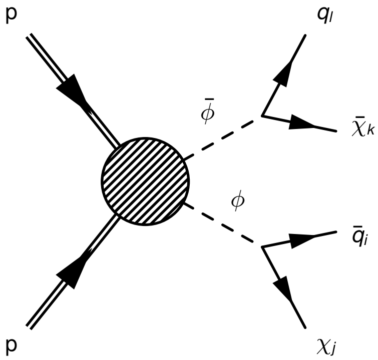

Figure : Studied LHC DM production processes.

Constraints from SUSY Searches at LHC

Involved QCD processes

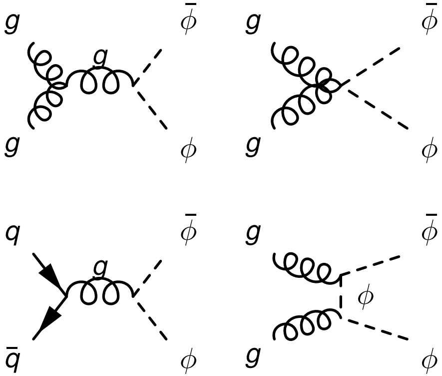

Involved NP processes

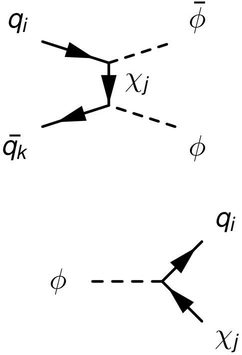

References

Constraints from $t\bar{t}+\not{E}_T$ Searches at LHC

- $D_{\lambda,33}$ increased
  $\rightarrow$ BR of decay goes up.
- $D_{\lambda,11}$, $D_{\lambda,22}$ increased
  $\rightarrow$ BR of decay goes down.

- **BUT**: For high $D_{\lambda,11} = D_{\lambda,22}$ we observe increasing excluded areas.

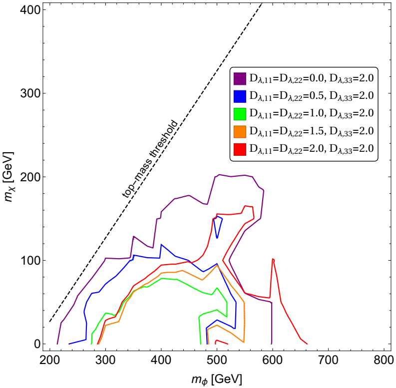

Figure : Exclusion plot for $t\bar{t}$ final state, mixing angles set to zero.

References

Constraints from SUSY Searches at LHC

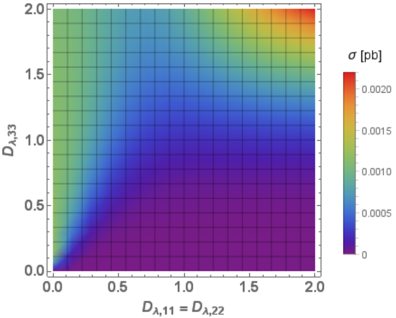

Figure : Cross section of $t\bar{t}$ final state for $m_\phi = 850$ GeV and $m_\chi = 50$ GeV, mixing angles set to zero.

Explanation: NP production

- Major contribution to total production (for high $D_{\lambda,11}$, $D_{\lambda,22}$)
- This effect can make up for drop in BR
- $D_{\lambda,33}$ not relevant, since the protons do not contain top
- Very high couplings can lead to serious exclusion areas.

Constraints from dijet + $\not{E}_T$ Searches at LHC

Karlsruhe Institute of Technology

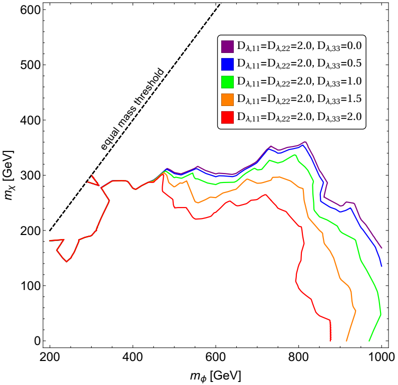

Figure : Exclusion plot for dijet final state, mixing angles set to zero.

- Stronger exclusion bounds on model.
- The phenomenologically interesting region is $m_\chi \leq 1$ TeV.
- Too large couplings $D_{\lambda,ii}$ would exclude nearly all of parameter space.
- Most serious constraints come from dijet final state.

$\Rightarrow$ Safe parameter-space:

$$m_\phi \geq 850 \text{ GeV}$$

$$2.0 \geq D_{\lambda,33} \geq D_{\lambda,22}, D_{\lambda,11}$$

Influence of Mixing Angles on LHC production

- Mixing angles shift influences between couplings $D_{\lambda,ii}$.
  $\Rightarrow$ For big splitting in the couplings, mixing angles can cause big shifts in cross sections.
- For our choice of m_ϕ bounds from $t\bar{t}$ final state cause no constraints.
- Worst allowed case for dijet final state, in our safe parameter-space, is $D_{\lambda,11} = D_{\lambda,22} = D_{\lambda,33} = 2.0$
  $\Rightarrow$ Unchanged by mixing angles.

$\Rightarrow$ Mixing angles can cause no problem with this choice of safe parameter-space.

Flavour Constraints from Neutral Meson Mixing

[UTfit collaboration '14]

- No mesons with top-quark are possible, the only constraints come from D-mesons.
  $\Rightarrow$ not too strong
- The NP contribution has to be smaller than experimental bounds.

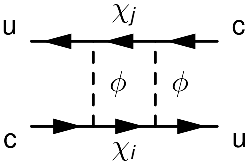

Figure : NP contr. to neutral D-meson mixing.

$$M_{12}^{D,NP} = \frac{1}{2m_D}\langle \bar{D}^0|\mathcal{H}_{eff}^{\Delta C=2,new}|D^0\rangle^* = \frac{1}{384\pi^2 m_\phi^2}\sum_{i,j}\lambda_{uj}^*\lambda_{cj}\lambda_{ui}^*\lambda_{ci}\cdot L(x_i,x_j)\cdot\eta_D\cdot m_D f_D^2\hat{B}_D.$$

Flavour Constraints from Neutral Meson Mixing

$$\left((\lambda\lambda^\dagger)_{cu}\right)^2 = \left((U_\lambda D_\lambda D_\lambda^\dagger U_\lambda^\dagger)_{cu}\right)^2$$

- For degeneracy $D_{\lambda,11} = D_{\lambda,22} = D_{\lambda,33}$ the mixing matrices U_{ij}^λ will drop out.
- The higher the splitting $\Delta_{ij} = D_{\lambda,ii} - D_{\lambda,jj}$, the more we will see the constraints on the mixing angle θ_{ij}.

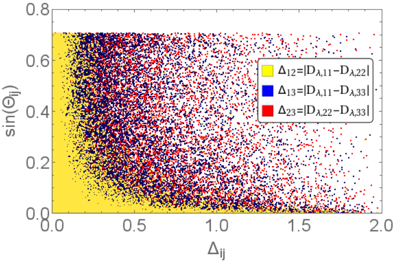

Figure : Valid mixing angles for different coupling splittings. $m_\phi = 850$ GeV and $m_\chi = 250$ GeV.

$\Rightarrow$ Most significant constraints on θ_{12}, other mixings nearly unconstrained.

References

DM Constraints from Observed Relic Abundance

[Steigman, Dasgupta, Beacom '12]

- Assume DM abundance as a thermal relic, $T_f \propto \frac{m_\chi}{20}$
- Co-annihilation CS has to be just large enough to produce the correct relic density (we allow for a 10% tolerance interval):

$$\langle \sigma v \rangle_{eff,exp} = 2.2 \times 10^{-26} \text{cm}^3/\text{s}.$$

$\Rightarrow$ cuts out valid area for $D_{\lambda,ii}$ depending on m_ϕ and m_χ

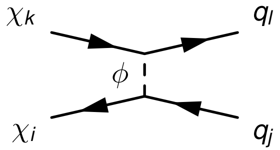

Figure : Co-annihilation of DM flavours.

$$\langle \sigma v \rangle_{eff} = \frac{1}{9} \times \frac{3}{256\pi} \sum_{i,j=1,2,3} \sum_{k,l=u,c,t} \lambda_{ki}\lambda^*_{ki}\lambda_{lj}\lambda^*_{lj} \frac{\sqrt{\left(4m_\chi^2 - (m_k - m_l)^2\right)\left(4m_\chi^2 - (m_k + m_l)^2\right)}}{\left(m_\phi^2 + m_\chi^2 - \frac{m_k^2}{2} - \frac{m_l^2}{2}\right)^2}.$$

DM Constraints from Observed Relic Abundance

- Depending on the mass splitting of the different DM flavours several freeze-out scenarios are possible.

$$m_{ij} = m_\chi(1 + \eta(D_{\lambda,ii})^2 + \ldots)\delta_{ij}.$$

- For a DM mass below the top-quark mass this decay channel drops out.

  $\Rightarrow$ CS formula and hence impact on parameters can be quite different

- Extreme example: only χ_t present at freeze-out with DM mass below top mass threshold:

$$\langle \sigma v \rangle_{eff} = \frac{3}{256\pi} \sum_{k,l=u,c} \lambda_{k3}\lambda_{k3}^*\lambda_{l3}\lambda_{l3}^* \frac{4m_\chi^2}{\left(m_\phi^2 + m_\chi^2\right)^2}.$$

Quasi-Degenerate Freeze-Out (QDF) Szenario

- All DM flavours are present at the freeze-out.
- We require the mass splitting to be less than 1% (significantly smaller than T_f) for this to happen.
- η is free parameter $\rightarrow$ choose it favourable: -0.01.
- This guarantees top-flavoured DM (see direct detection section for motivation).
- Constraint cuts out valid area for $D_{\lambda,ii}$ depending on m_ϕ and m_χ.
- Lower bound on m_χ due to upper limits for $D_{\lambda,ii}$, depending on m_ϕ.

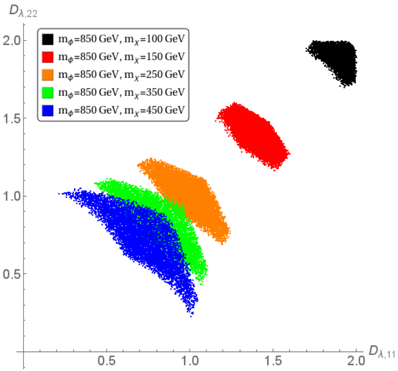

Figure : Valid points in quasi-degenerate freeze-out scenario.

Single Flavour Freeze-Out (SFF) Szenario

- Only m_χ present at freeze-out.
- We require the mass splitting to be more than 10% (significantly bigger than T_f) for this to happen.
- η is free parameter $\rightarrow$ choose it favourable: -0.075.
- This guarantees top-flavoured DM (see direct detection section for motivation).
- Constraint cuts out valid area of parameters depending on m_ϕ and m_χ, with significant effect on mixing angles.
- In addition to lower bound, we also find an upper bound on m_χ due to upper and lower (from mass splitting condition) limits for $D_{\lambda,ii}$, depending on m_ϕ.

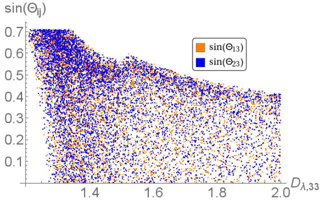

Figure : Valid points in single flavour freeze-out scenario for $m_\phi = 850$ GeV and $m_\chi = 210$ GeV.

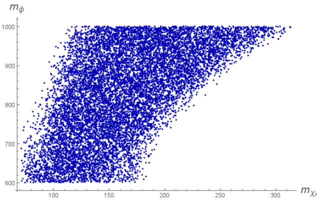

Figure : Mass bounds in single flavour freeze-out scenario.

DM Bounds from Direct Detection Experiments

Many contributions to total WIMP-nucleon cross section:

$$\sigma_n^{SI} = \frac{\mu_n^2}{\pi A^2} |Zf_p + (A - Z)f_n|^2.$$

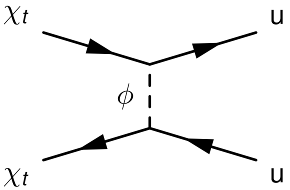

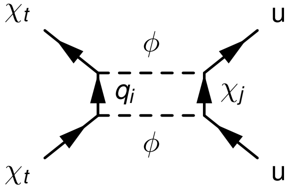

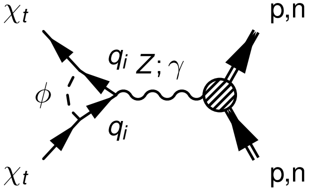

DM Bounds from Direct Detection Experiments

$$f_p^{tree} = 2f_n^{tree} = \frac{|\lambda_{ut}|^2}{4m_\phi^2}.$$

$$f_p^{box} = 2f_n^{box} = \sum_{i,j} \frac{|\lambda_{ui}|^2|\lambda_{jt}|^2}{32\pi^2 m_\phi^2} F\left(\frac{m_{q_i}^2}{m_\phi^2}, \frac{m_{\chi_j}^2}{m_\phi^2}\right).$$

$$f_p^{photon} = -\sum_i \frac{|\lambda_{it}|^2 e^2}{48\pi^2 m_\phi^2}\left(\frac{3}{2} + log\left(\frac{m_{q_i}^2}{m_\phi^2}\right)\right).$$

$$f_p^Z = -\sum_i \frac{3|\lambda_{it}|^2 e^2\left(\frac{1}{2} - 2sin^2(\Theta_W)\right)}{32\pi^2 sin^2(\Theta_W)cos^2(\Theta_W)m_Z^2}\frac{m_{q_i}^2}{m_\phi^2}\left(1 + log\left(\frac{m_{q_i}^2}{m_\phi^2}\right)\right).$$

$$f_n^Z = -\sum_i \frac{3|\lambda_{it}|^2 e^2\left(-\frac{1}{2}\right)}{32\pi^2 sin^2(\Theta_W)cos^2(\Theta_W)m_Z^2}\frac{m_{q_i}^2}{m_\phi^2}\left(1 + log\left(\frac{m_{q_i}^2}{m_\phi^2}\right)\right).$$

DM Bounds from Direct Detection Experiments

[LUX collaboration '15]

- All contributions have to combine to a WIMP-nucleon cross-section below the LUX bounds.
- All contributions are positive, only the Z-penguin with the neutron is negative $\Rightarrow$ saves the day.
- Largest contribution comes from tree-level process. Largest negative term is hence interference term of tree-level and neutron Z-penguin.
- Most important terms, have to nearly cancel each other:

$$A_{\mathcal{I}} \cdot D^4_{\lambda,33} \cdot sin(\theta_{13})^4 - A_{\mathcal{I}\mathcal{I}} \cdot D^4_{\lambda,33} \cdot sin(\theta_{13})^2 \cdot cos(\theta_{13})^2 \cdot cos(\theta_{23})^2$$

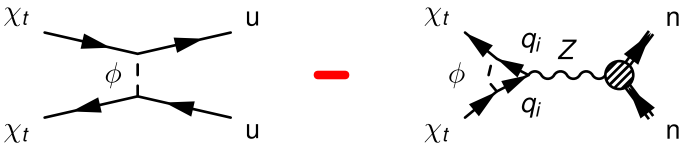

Figure : Cancellation of tree-level and neutron Z-penguin contributions (symbolic).

DM Bounds from Direct Detection Experiments

- Tree level and neutron Z-penguin have to nearly cancel each other.
  $\Rightarrow$ serious constraints on θ_{13}
- For higher couplings the cancellation gets more complicated.
- For too large couplings the cancellation is no longer possible at all
  $\rightarrow$ excluded.
- Top-flavoured DM is the natural choice:
  $\Rightarrow$ Tree-level contribution small
  $\Rightarrow$ Neutron Z-penguin contribution large.

Figures/QDF_onlyDD_phi850

Figure : Valid mixing angle Θ_{13} vs $D_{\lambda,33}$.

Combined Analysis of Constraints (QDF)

Combined application of both flavour, relic abundance and direct detection constraint in quasi-degenerate freeze-out scenario.

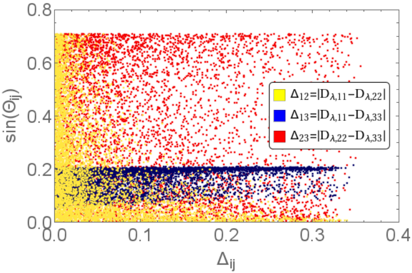

Figure : Valid points for $m_\phi = 850$ GeV and $m_\chi = 150$ GeV (QDF).

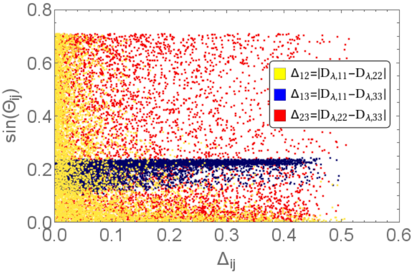

Figure : Valid points for $m_\phi = 850$ GeV and $m_\chi = 250$ GeV (QDF).

Combined Analysis of Constraints (QDF)

- A combination of relic abundance and direct detection constraints confine θ_{13} to a narrow interval.
- The bounds on the DM mass become more serious, since the parameters do not only have to fulfill relic abundance constraints.
- The combined analysis clearly prefers top-flavoured DM.

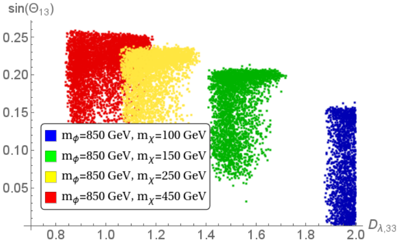

Figure : Valid points in θ_{13}-$D_{\lambda,33}$-plane (QDF).

Combined Analysis of Constraints (SFF)

Combined application of both flavour, relic abundance and direct detection constraint in single flavour freeze-out scenario.

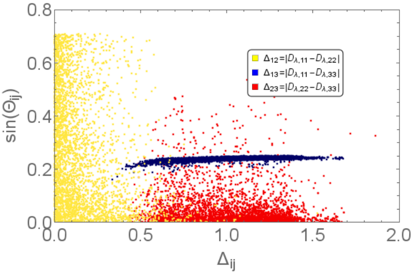

Figure : Valid points for $m_\phi = 850$ GeV and $m_\chi = 225$ GeV (SFF).

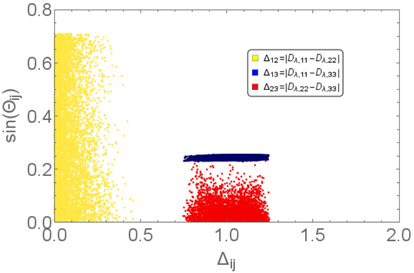

Figure : Valid points for $m_\phi = 850$ GeV and $m_\chi = 250$ GeV (SFF).

Combined Analysis of Constraints (SFF)

- A combination of relic abundance and direct detection constraints confine θ_{13} to a narrow interval (even more serious than in QDF).
- Especially in SFF the combination of all constraints extremely limits the chance of finding a valid configuration of all parameters for $m_{\chi_t} \leq m_{top}$.
- The combined analysis clearly prefers top-flavoured DM.

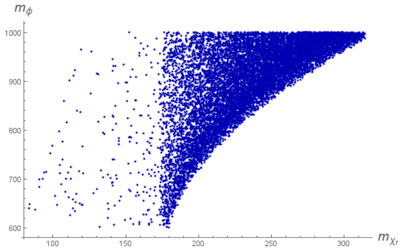

Figure : Valid points in mass plot for combined constraints (SFF).

Backup Material 1

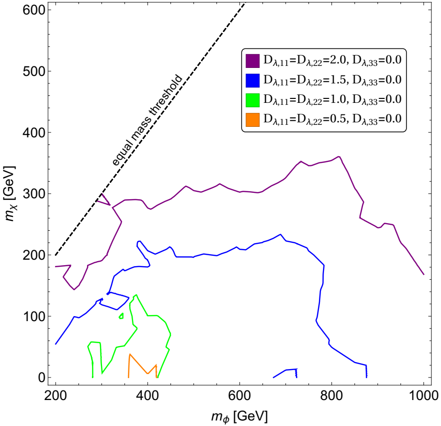

Figure : Exclusion plots for dijet final state for various couplings, mixing angles set to zero.

Backup Material 2

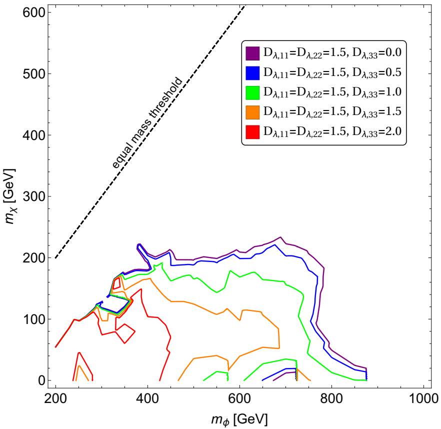

Figure : Exclusion plots for dijet final state for various couplings, mixing angles set to zero.

Backup Material 3

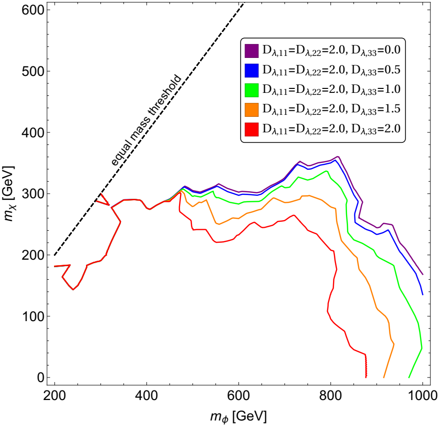

Figure : Exclusion plots for dijet final state for various couplings, mixing angles set to zero.

Backup Material 4

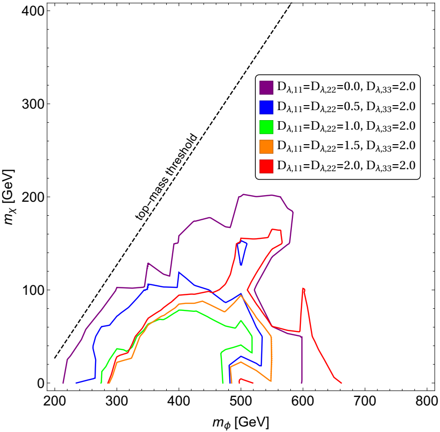

Figure : Exclusion plots for $t\bar{t}$ final state for various couplings, mixing angles set to zero.

Backup Material 5

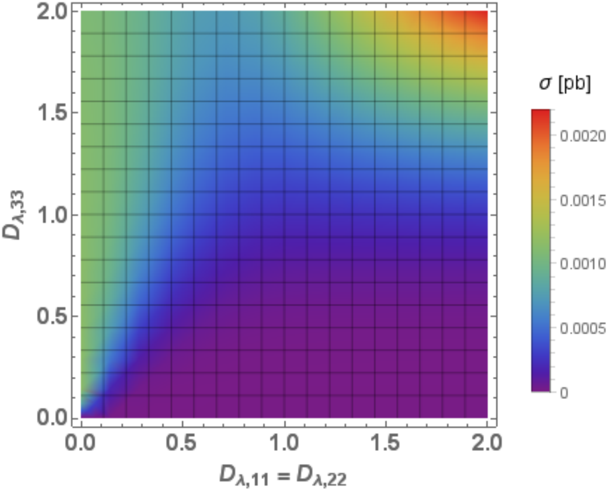

Figure : Cross section for $t\bar{t}$ final state, mixing angles set to zero.

Backup Material 6

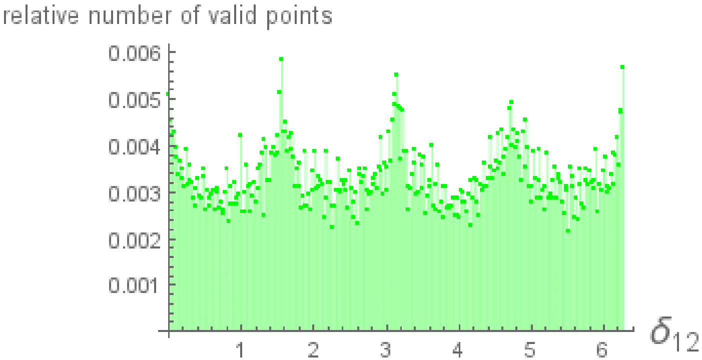

Figure : Impact of flavour constraints on Θ_{12}.

Backup Material 7

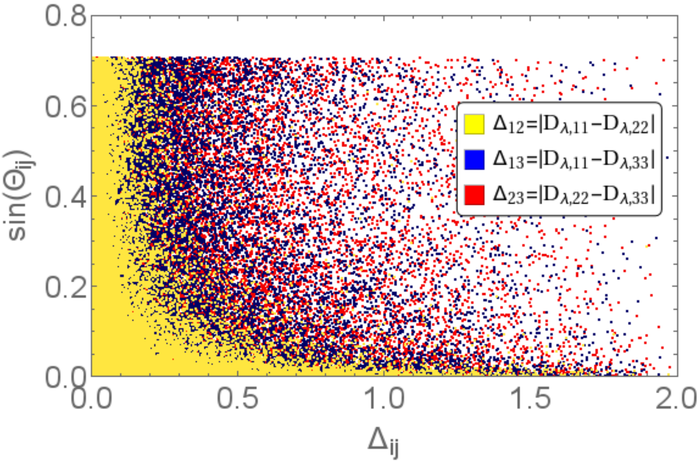

Figure : Valid mixing angles for different coupling splittings. $m_\phi = 850$ GeV and $m_\chi = 250$ GeV.

Backup Material 8

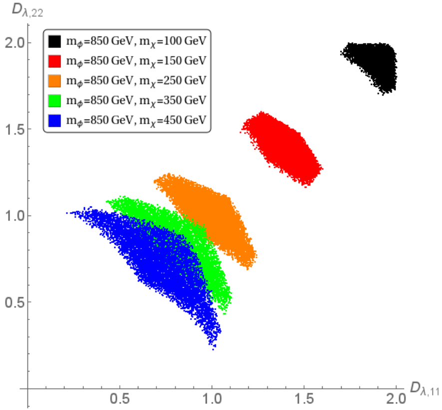

Figure : Valid points in quasi-degenerate freeze-out scenario in $D_{\lambda,11} - D_{\lambda,22}$-plane for various DM masses.

Backup Material 9

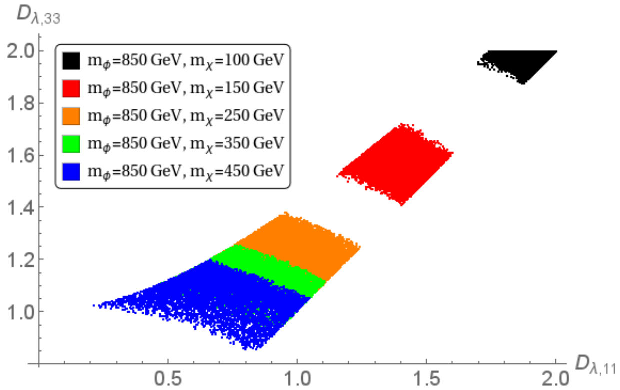

Figure : Valid points in quasi-degenerate freeze-out scenario in $D_{\lambda,11} - D_{\lambda,33}$-plane for various DM masses.

Backup Material 10

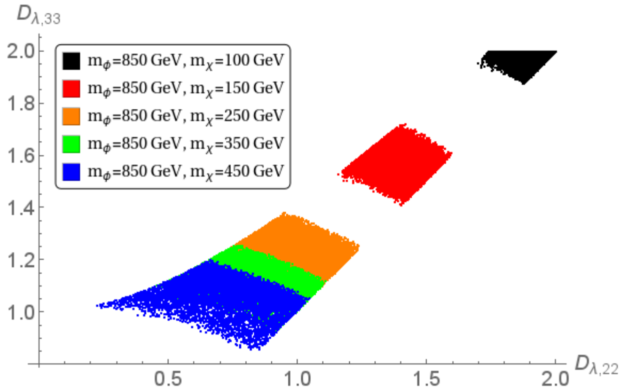

Figure : Valid points in quasi-degenerate freeze-out scenario in $D_{\lambda,22} - D_{\lambda,33}$-plane for various DM masses.

Backup Material 11

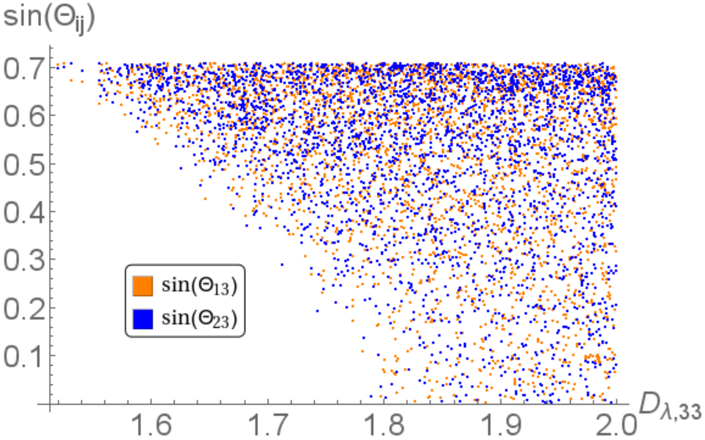

Figure : Valid points in single-flavour freeze-out scenario in $D_{\lambda,33} - \sin(\Theta_{ij})$-plane for $m_\phi = 850$ GeV and $m_\chi = 150$ GeV.

Backup Material 12

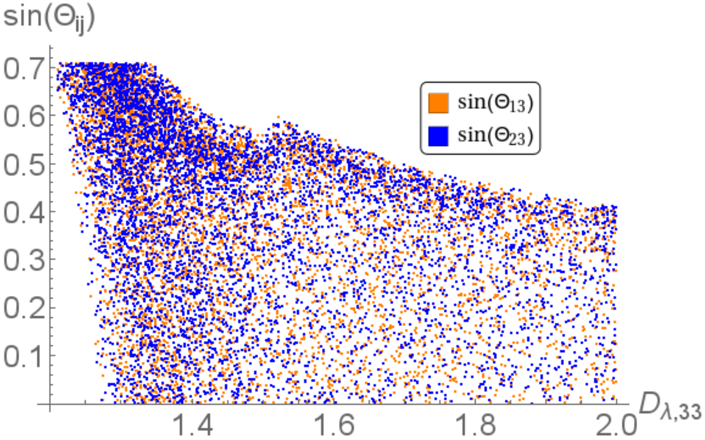

Figure : Valid points in single-flavour freeze-out scenario in $D_{\lambda,33} - \sin(\Theta_{ij})$-plane for $m_\phi = 850$ GeV and $m_\chi = 210$ GeV.

Backup Material 13

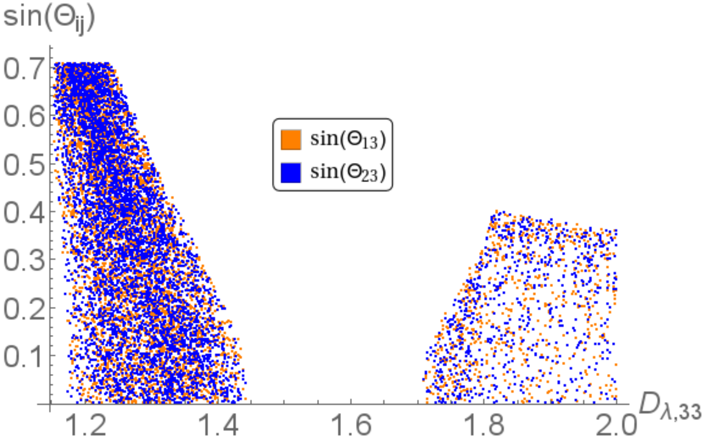

Figure : Valid points in single-flavour freeze-out scenario in $D_{\lambda,33} - \sin(\Theta_{ij})$-plane for $m_\phi = 850$ GeV and $m_\chi = 230$ GeV.

Backup Material 14

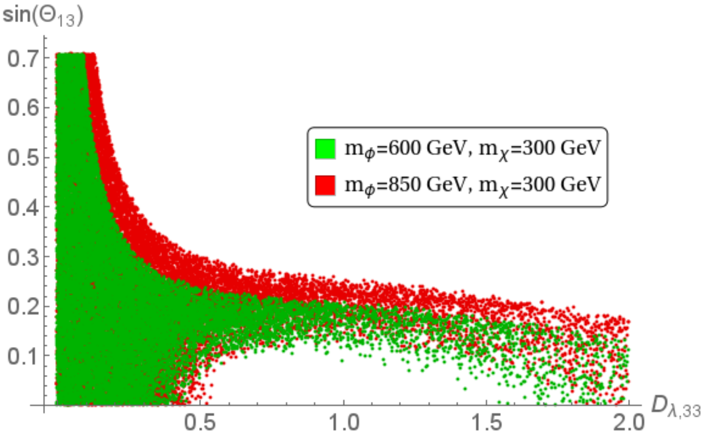

Figure : Valid points for LUX bounds in $D_{\lambda,33} - \sin(\Theta_{13})$−plane.

Backup Material 15

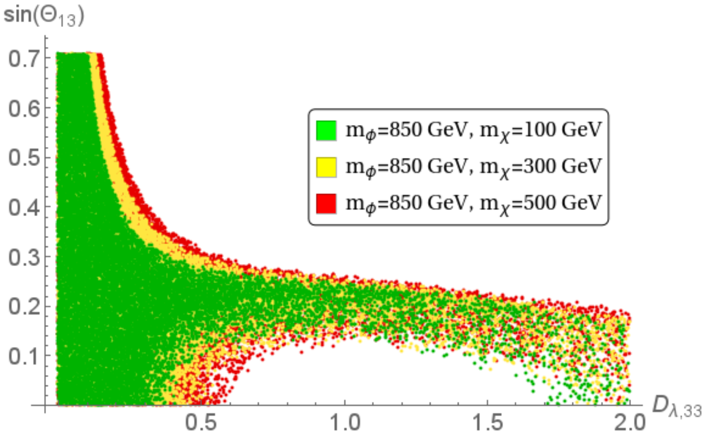

Figure : Valid points for LUX bounds in $D_{\lambda,33} - \sin(\Theta_{13})-$plane.

Backup Material 16

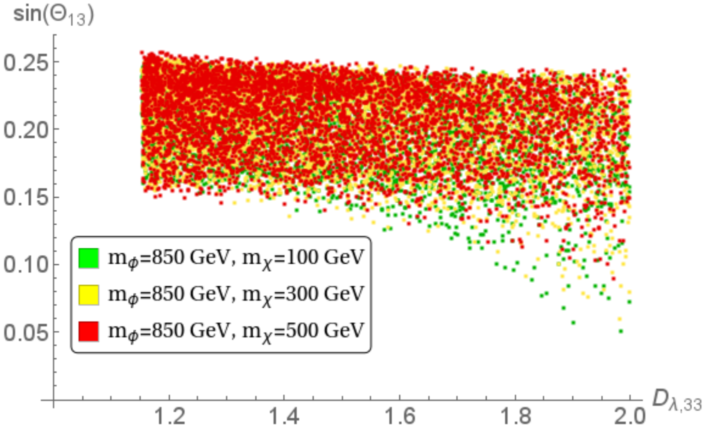

Figure : Valid points for LUX bounds in $D_{\lambda,33} - \sin(\Theta_{13})-$plane, with SFF splitting applied.

Backup Material 17

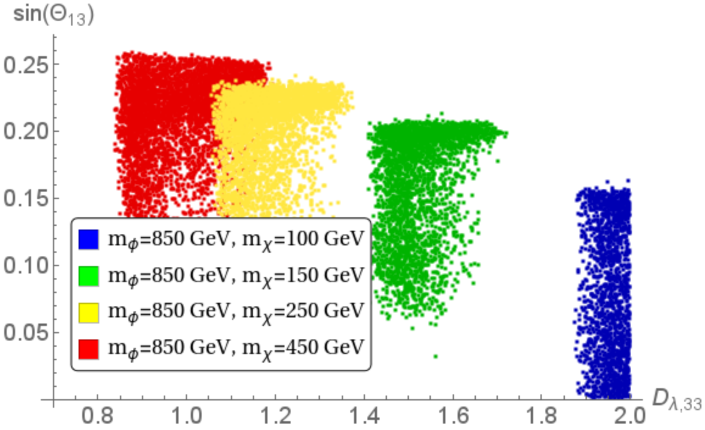

Figure : Valid points of combined analysis for quasi-degenerate freeze-out scenario in $D_{\lambda,33} - \sin(\Theta_{13})$−plane for different DM masses.

Backup Material 18

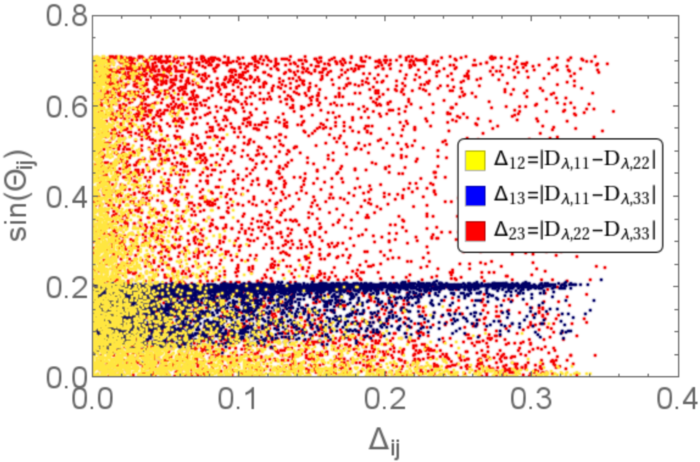

Figure : Valid mixing angles for different coupling splittings for quasi-degenerate freeze-out scenario. $m_\phi = 850$ GeV and $m_\chi = 150$ GeV.

Backup Material 19

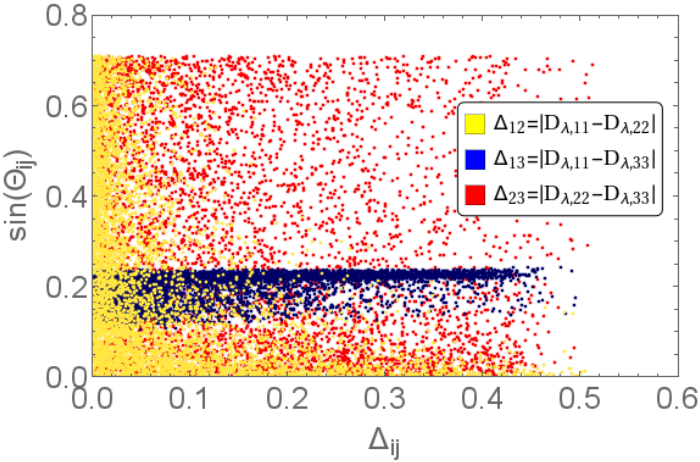

Figure : Valid mixing angles for different coupling splittings for quasi-degenerate freeze-out scenario. $m_\phi = 850$ GeV and $m_\chi = 250$ GeV.

Backup Material 20

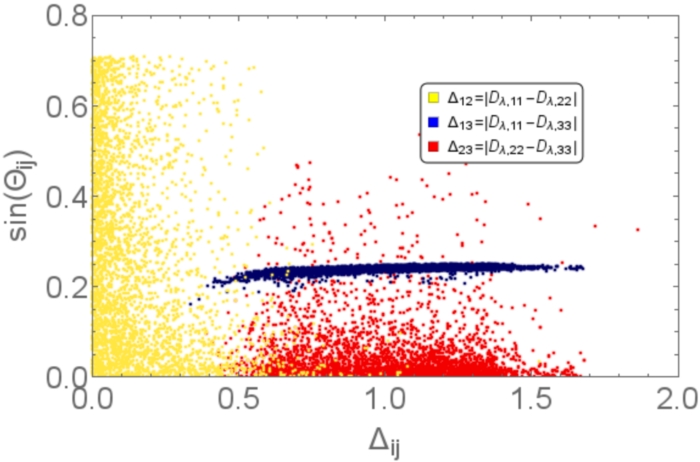

Figure : Valid mixing angles for different coupling splittings for single-flavour freeze-out scenario. $m_\phi = 850$ GeV and $m_\chi = 225$ GeV.

Backup Material 21

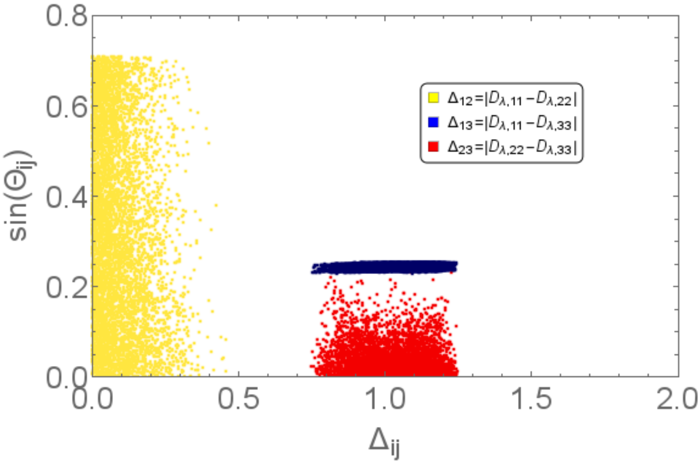

Figure : Valid mixing angles for different coupling splittings for single-flavour freeze-out scenario. $m_\phi = 850$ GeV and $m_\chi = 250$ GeV.